Structural Studies on Solvates of Cyclic Imide Tethered Carboxylic Acids with Pyridine and Quinoline

3 AUTHORS:

Devendra Singh
nothing

12 PUBLICATIONS **77** CITATIONS

SEE PROFILE

Pradip Kr. Bhattacharyya
Ayra vidyapeeth College

40 PUBLICATIONS **79** CITATIONS

SEE PROFILE

Jubaraj B Baruah
Indian Institute of Technology Guwahati

252 PUBLICATIONS **2,047** CITATIONS

SEE PROFILE

Structural Studies on Solvates of Cyclic Imide Tethered Carboxylic Acids with Pyridine and Quinoline

Devendra Singh,[†] Pradip K. Bhattacharyya,[‡] and Jubaraj B. Baruah*,[†]

[†]*Department of Chemistry, Indian Institute of Technology Guwahati, Guwahati 781 039 Assam, India, and* [‡]*Department of Chemistry, Arya Vidyapeeth College, Guwahati-16, Assam*

ABSTRACT: Structures of eight solvates of cyclic imide tethered carboxylic acids and aromatic tetra carboxylic acids with pyridine (solvate **I−VI**) and quinoline (**VII−VIII**) are determined. Different types of hydrogen bond motifs (discrete or cyclic) in these solvates are identified. Solvates **I** and **II** possess discrete O−H···N interactions, solvates **III** and **VIII** possess combinations of cyclic interactions arising from O−H···N and C−H···O interactions, solvates **IV**, **V**, and **VII** have both the above namely discrete and cyclic types of interactions, whereas, solvate **VI** is an exception which possesses discrete O−H···N as well as $R^2_2(8)$ types of interactions and provides a model system for incomplete cleavage of dimeric assembly of carboxylic acid moiety. On the basis of the results of various hydrogen bond motifs, density functional theory calculations (DFT) on similar motifs generated from formic acid and its interaction with pyridine and quinoline are carried out. In the case of a pyridine formic acid system, DFT calculations show that the energy difference between the cyclic $R^2_2(7)$ motif and the discrete motif is ∼0.6 kcal/mol. Such a small difference accounts for the formation of both types of structural patterns in solvates **I−V** depending on the steric requirements. The observed motif of **VI** is established by comparison of theoretical energies between a dimeric carboxylic acid moiety generated from two formic acids interactions and a trimeric moiety that exhibits two formic acids and pyridine interactions. The energy of different types of hydrogen bond motifs formed by the interactions between quinoline and formic acid is also calculated. Calculations based on DFT show that the salt formation between formic acid and pyridine is not a favorable process, but it may occur in the case of quinoline.

Introduction

The interactions of carboxylic acids with pyridine and related nitrogen containing heterocyclic compounds are well studied.[1] The knowledge of these interactions is useful in pharmceuticals,[2] and also in the synthesis of porous materials.[3] The hydrogen bonds between carboxylic acids and simple aromatic amines may be of different types.[4] Some possible hydrogen bond motifs arising from interactions of carboxylic acid with pyridine and quinoline are shown in Figure 1, and some of those motifs are already available in the literature.[1a,4] Steric factors play an important role in stabilization of these motifs.[5] Depending on the association of parent carboxylic acids in cyclic hydrogen bonds, it is likely that such hydrogen bond motifs may originate from cleavage of cyclic dimeric carboxylic acid by inclusion of a base such as pyridine or quinoline. The validity of such observations can be checked if it is possible to identify motifs such as PyA3 as illustrated in Figure 1. In addition, depending on the packing effect[6] as well as pK_a of an acid and a base,[1a,7] the hydrogen bonded assembly of amines with carboxylic acids leads to formation of either solvates or salts. The effect of pK_a on such processes is reported in detail in the literature.[7c] The R groups considered in the present study are either aromatic ring or aromatic rings attached through a C−N bond to phthalimide or naphthalimide. It is anticipated that the free rotation of such phthalimide or naphthalimide aromatic rings around the C−N bond would provide an environment to adjust hydrogen bond motifs with geometry guided by the dipolar nature of the phthalimide or naphthalimide rings.[8] Further, it may be noted

that the two carbonyl groups of the imide would participate in weak interactions to guide the orientation of the carboxylic acid groups.

Thus, to establish these motifs (as shown in Figure 1) in solid-state assembly, we have studied the structures of solvates of pyridine/quinoline of aromatic tetracarboxylic acid, and some of the carboxylic acids that are tethered by phthalimide or naphthalimide. The compounds used in this study for preparation of solvates are shown in Figure 2. Analogous motifs derived from interactions of pyridine or quinoline with formic acid were constructed and their corresponding energies were calculated by density functional theory (DFT) using diffuse functions.[9]

Results and Discussion

The solvates of compounds **1−6** with pyridine (**I−VI**) were prepared and characterized (Scheme 1). The structure of all these pyridine solvates were determined and salt formation was not observed in any case. The 1:1 (carboxylic acid/pyridine) stoichiometry of the hydrogen bond donor to acceptor was found in the solvates and the structure of each solvate exhibits O−H···N interactions. Part of the crystal structures of pyridine solvates **I−V** is shown in Figure 3 and the hydrogen bond parameters are listed in Table 1.

In solvate **I** (1:1 solvate) pyridine molecule is associated with the carboxylic acid via O−H···N interactions as a discrete hydrogen bond, the molecules of pyridines and the acids in the lattice also form an assembly through C5−H···O3 (d_{d-A}, 3.18 Å, and ∠A−H···D, 132.1°) and C18−H···O4 (d_{d-A}, 3.38 Å, and ∠A−H···D, 137.1°) interactions. The solvate **II** is analogous to solvate **I**, and in this case also we observed discrete hydrogen bonds between

*To whom correspondence should be addressed. E-mail: juba@iitg.ernet.in.

Table 1. Hydrogen Bond Geometry (Å, °) for the Solvates I−V

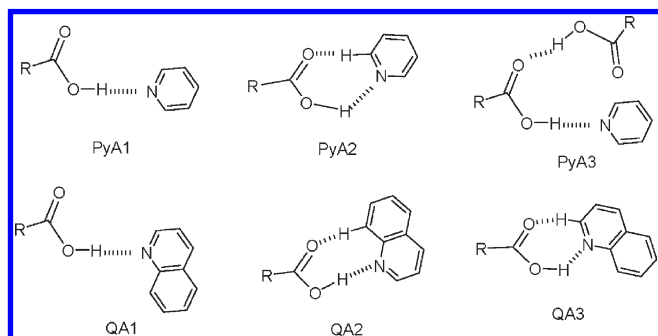| compounds	D−H⋯A	d (D−H)	d (H⋯A)	d (D⋯A)	∠D−H⋯A
I	O4−H4A⋯N2 [x, $-y + 3/2$, $z + 1/2$]	0.82	1.85	2.66	174.2
II	O4−H4A⋯N2	0.82	1.77	2.58	169.7
III	O2−H2A⋯N2 [$-x + 1/2$, $y + 1/2$, $-z$]	0.82	1.82	2.63	174.0
IV	O1−H1⋯N2 [$-x + 1$, $-y + 1$, $-z$]	0.82	1.84	2.65	175.4
	O7−H7⋯N4 [$x - 1$, $y - 1$, z]	0.82	1.83	2.65	175.0
	O4−H4A⋯N3 [$x - 1$, y, z]	0.82	1.75	2.56	166.5
V	O4−H4⋯N1 [x, $-y + 3/2$, $z + 1/2$]	0.82	1.78	2.57	161.7
	O1−H1⋯N2	0.82	1.77	2.59	173.6

Figure 1. Some hydrogen bonded motifs from interactions of pyridine and quinoline with a carboxylic acid.

pyridine and carboxylic acid group. The pyridine molecules are further held by C−H⋯O interactions, namely, C29−H⋯O2 (d_{d-A}, 3.12 Å, and ∠A−H⋯D, 109.7°) and C32−H⋯O2 (d_{d-A}, 3.45 Å, and ∠A−H⋯D, 140.7°) and C−H⋯π interactions ($d_{C15\cdots\pi}$, 3.59 Å) in the assembly.

In solvate **III** (1:2 solvate), a cyclic $R^2_2(7)$ type of hydrogen bond pattern is observed between the pyridine molecules and carboxylic acid groups. Both the pyridine molecules present in **III** are involved in cyclic type of hydrogen bonding with the dicarboxylic acid via O−H⋯N [O2−H2A⋯N2 (d_{d-A}, 2.63 Å, and ∠A−H⋯D, 174.0°)] as well as C−H⋯O [C11−H11⋯O3 (d_{d-A}, 3.27 Å, and ∠A−H⋯D, 125.7°)] interactions. Moreover, the pyridine molecules are also associated in the lattice via C−H⋯O interactions, namely, C12−H12⋯O1 (d_{d-A}, 3.30 Å, and ∠A−H⋯D, 131.8°) and C13−H13⋯O3 (d_{d-A}, 3.41 Å, and ∠A−H⋯D, 136.3°) with dicarboxylic acid molecules.

In solvate **IV** (1:3 solvate), both cyclic $R^2_2(7)$ and discrete types of hydrogen bond patterns are observed. Two pyridine molecules are involved in cyclic type of hydrogen bonding with carboxylic acid groups via O−H⋯N [O1−H1⋯N2 (d_{d-A}, 2.65 Å, and ∠A−H⋯D, 175.4°) and O7−H7⋯N4 [(d_{d-A}, 2.65 Å, and ∠A−H⋯D, 175.0°)] as well as C−H⋯O [C21−H21⋯O8 (d_{d-A}, 3.27 Å, and ∠A−H⋯D, 126.0°) and C30−H30⋯O2 (d_{d-A}, 3.16 Å, and ∠A−H⋯D, 126.1°) interactions, whereas one pyridine molecule is associated with a carboxylic acid group through a discrete type of O−H⋯N interaction, namely, O4−H4⋯N3 (d_{d-A}, 2.56 Å, and ∠A−H⋯D, 166.5°) interaction. Moreover, both types of pyridine molecules involving in cyclic and discrete hydrogen bondings are also held in the crystal lattice via C−H⋯O interactions, namely, C18−H18⋯O6 (d_{d-A}, 3.41 Å, and ∠A−H⋯D, 143.9°) and C29−H29⋯O6 (d_{d-A}, 3.36 Å, and ∠A−H⋯D, 143.9°) interactions respectively and further interact to each other via C−H⋯π interactions ($d_{C19\cdots\pi}$, 3.59 Å) in the assembly.

In solvate **V** (1:4 solvate) the four carboxylic acid groups of naphthalene-1,4,5,8-tetracarboxylic acid are in a sterically crowded environment, and they are expected to be in a
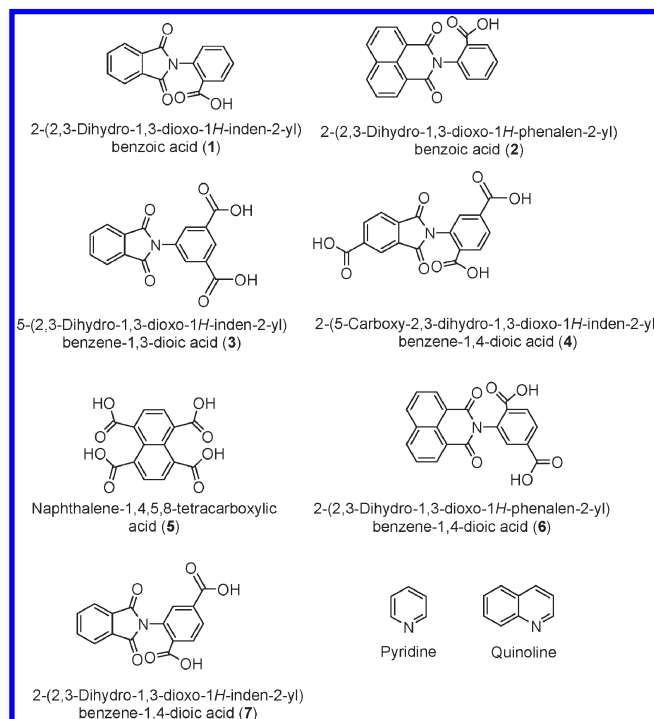

Figure 2. Structure of different compounds studied.

nonplanar orientation. Both the discrete and cyclic types of hydrogen bond patterns are also observed in this solvate. Two carboxylic acid groups present on each side of the naphthalene ring interact with two pyridine molecules via discrete O−H⋯N interactions as well as a combination of cyclic O−H⋯N and C−H⋯O interactions, respectively. Both the discrete and cyclic hydrogen bonded pyridine molecules are positioned in trans orientation to each other around the naphthalene ring, and a cyclic hydrogen bond pattern is formed via O4−H4⋯N1 and C11−H11⋯O3 interactions.

Since different types of hydrogen bond motifs are observed in the structures of solvates **I−V**, we performed DFT calculations on analogous motifs constructed from formic acid and pyridine. Optimized structures of pyridine/formic acid motifs at the B3LYP/6-31+G* level of theory are shown in Figure 4. In structure **4a**, both the formic acid and pyridine molecules are coplanar (with a dihedral angle H−O−C−O = 0° in formic acid), which facilitates the formation of two short-range interactions viz. O−H⋯N ($d_{H\cdots A}$, 1.73 Å) and C−H⋯O ($d_{H\cdots A}$, 2.45 Å) interactions. However, in the case of the structure **4b**, the two molecules lie at an angle 90° to each other, which allows the formation of only one O−H⋯N ($d_{H\cdots A}$, 1.78 Å) interaction, and consequently the structure **4b** is found to be less stable than **4a**. To obtain a optimized structure with pyridine/formic acid at an angle 90° to each other, as shown in Figure 4b, we use H−O−C−O = 180°, and the calculated energy difference between the two conformers
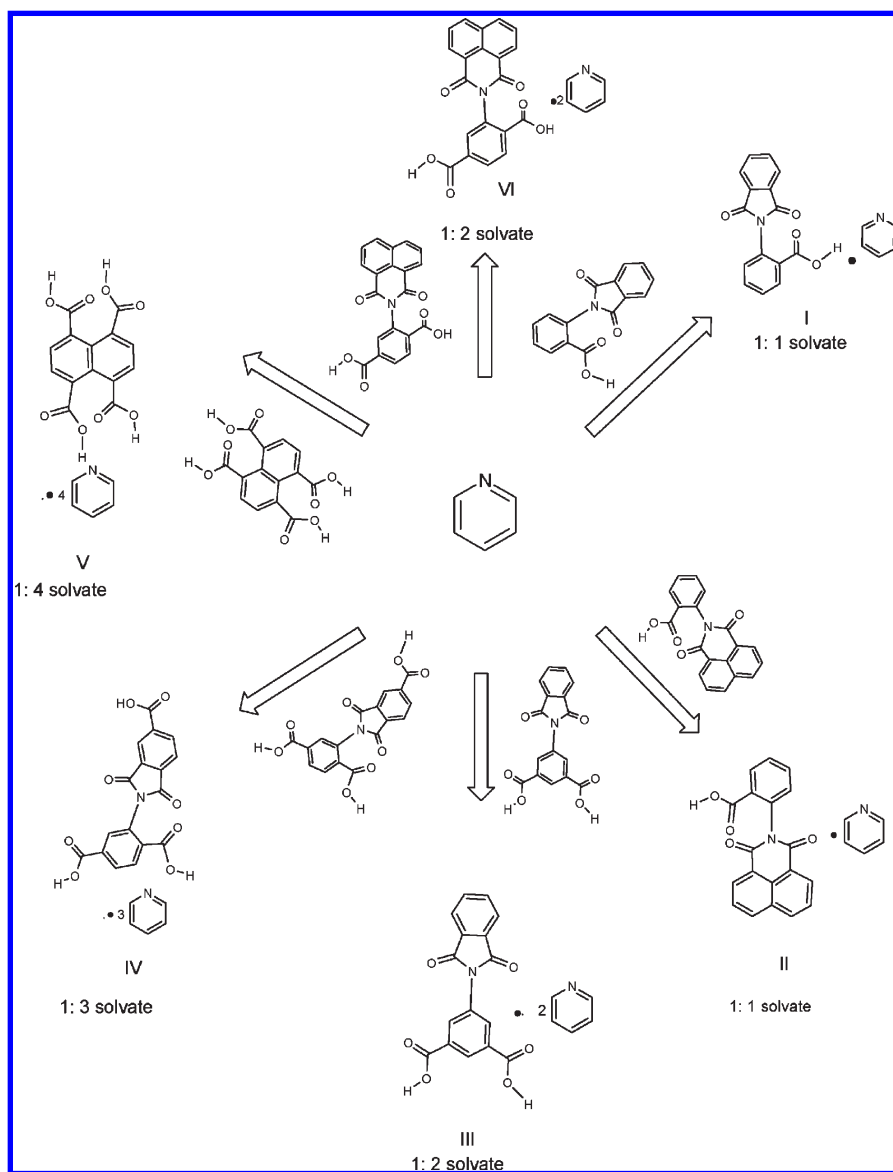
Scheme 1. Various Solvates of Pyridine

Table 2. Stability of 4a with Different Basis Sets (in kcal/mol)

basis sets	relative stability of **4a**
6-31+G*	−0.16
6-31++G*	−0.13
6-31++G**	−0.31
AUG-cc-pVDZ	−0.61

of the acid molecule (with H−O−C−O = 0° and with H−O−C−O = 180°) and subtracted it from the interaction energy of **4b** to obtain relative stability of **4a** ($E_{4a} - E_{4b}$) because a stable structure like **4a** was obtained only when the formic acid was used with H-O-C-O = 0°. Relative stability of **4a** calculated with different basis functions is shown in Table 2. It is observed that with lower level basis functions, the relative stability of **4a** is found to be ∼0.15 kcal/mol, whereas highly polarization and diffuse basis function, 6-31++G** gives this value −0.31 kcal/mol. Diffuse double-ζ basis function AUG-cc-pVDZ shows the highest relative stability, that is, −0.61 kcal/mol. The importance of such small interaction energies in crystal lattice is well documented.[1f]

Such a small difference in energy[1f] accounts the probability of both the structures depicted in Figure 4. The solvates **I** and

II have discrete types of hydrogen bonds, whereas the solvate **III** has a cyclic type and the solvates **IV−V** have both types; these results combined with the narrow energy differences between the cyclic and discrete structure suggest that the interplay of these weak interactions occurs in the packing pattern and such an effect with steric requirements decide the formation of different types of hydrogen bond motifs in the solid-state structures of these systems.

As mentioned in the introduction, there is a need to understand the origin of these motifs, and one of such model may be formed from a dimeric carboxylic acid with $R^2_2(8)$ type hydrogen bond motif as illustrated in Scheme 2. This motif indicates a path involving dissociation of carboxylic acid dimer by pyridine molecule to form an assembled structure between two carboxylic acids and one pyridine molecule. However, stability of such a motif is governed by a synergic effect to control the approach of a pyridine molecule to an optimum distance of dimeric carboxylic acid unit, so that it does not cross a limiting value to make a monomeric 1:1 solvate. A system that would be appropriate for such process can be imagined as a system in which the pyridine molecules are held by C−H···O interactions from the back side of the
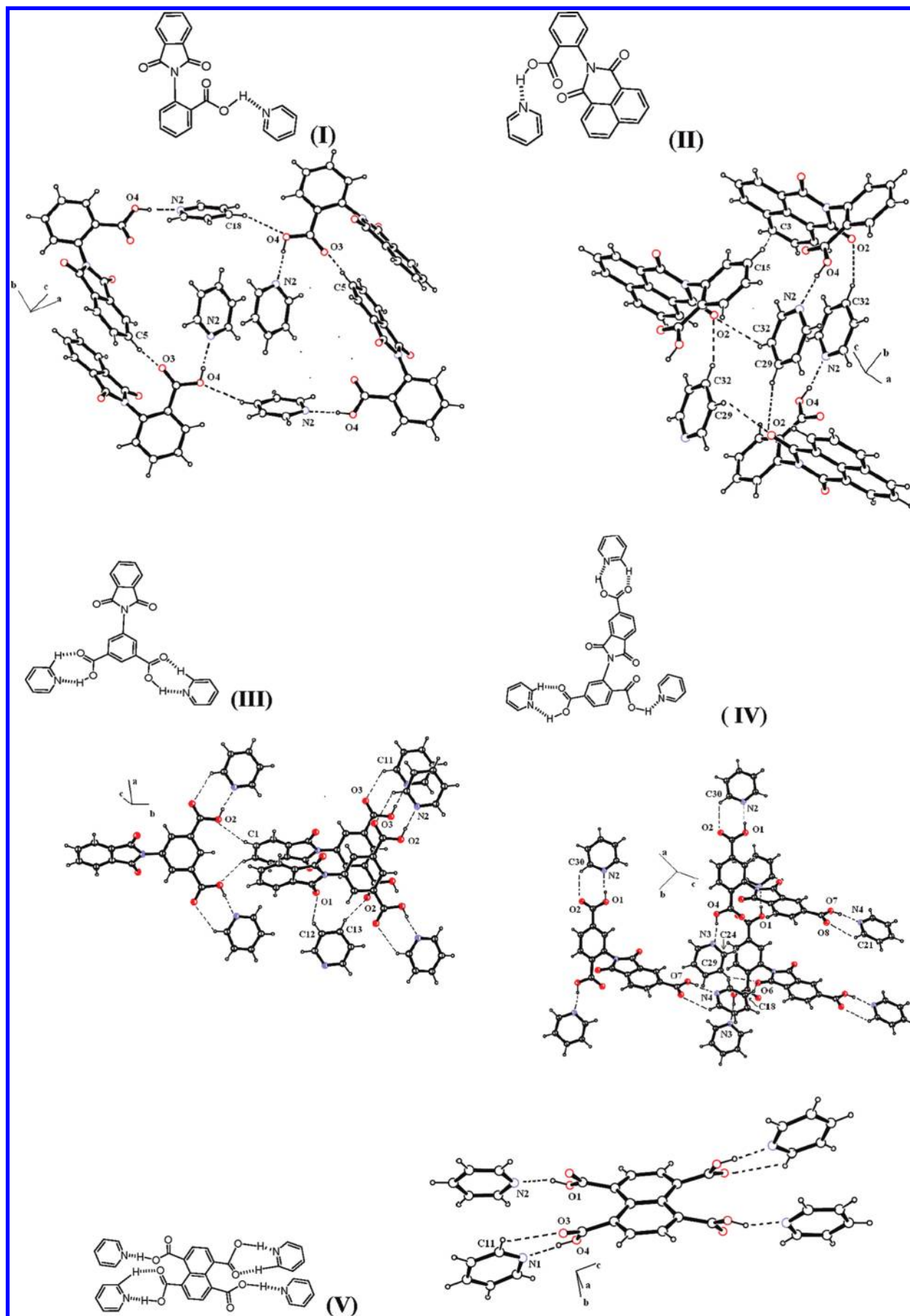
Figure 3. Part of the crystal structures of solvates (**I−V**) showing weak interactions among carboxylic acids and pyridine (drawn with 20% thermal ellipsoid).

Table 3. Hydrogen Bond Geometry (Å, °) for the Solvate VI

D−H···A	d(D−H)	d(H···A)	d(D···A)	∠D−H···A
O2−H2···O4 [$x + 1/2, y + 1/2, z$]	0.82	1.70	2.51	171.0
O3−H3A···N2 [$x, y − 1, z$]	0.82	1.88	2.57	150.9

Scheme 2. Assembly Formation between Two Carboxylic Acid Molecules and a Pyridine Molecule

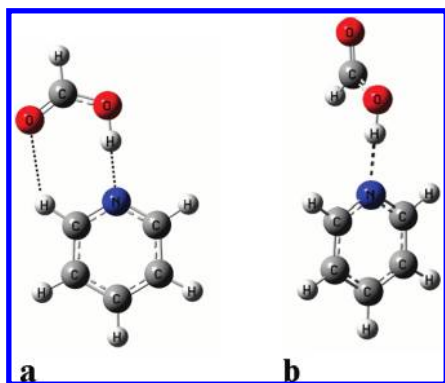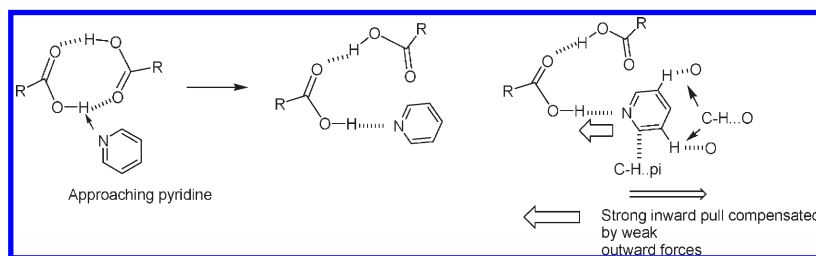**Figure 4.** (a, b) The optimized structures pyridine/formic acid motifs at two different orientations.

O−H···N interactions so that a pyridine is held by a pull from the back, as illustrated in Scheme 2.

The structure of a 1:2 solvate of compound **6** with pyridine (solvate **VI**) provides a model system for such incomplete cleavage of dimeric assembly of the carboxylic acid moiety. Solvate **VI** is associated with discrete O−H···N as well as $R^2_2(8)$ type of interactions. Other weak interactions such as C23−H···O3 ($d_{d\text{-}A}$, 3.18 Å, and ∠A−H···D, 122.5°), C22−H···O6 ($d_{d\text{-}A}$, 3.17 Å, and ∠A−H···D, 133.7°), and C3−H···π ($d_{C3\ldots\pi}$, 3.79 Å) interactions and relatively strong π···π interactions (d_{C3-C4}, 3.39 Å) between the aromatic ring containing the carboxylic acids are also present in the part of the crystal structure (Table 3, Figure 5).

To follow the feasibility of formation of PyA3 type of motif as illustrated in Figure 1, which is also the motif seen in solvate **VI**, we have calculated the interaction energy of a formic acid dimer and the effect of presence of one pyridine molecule on acid dimer. The optimized structures of the two systems at B3LYP/6-31+G* level of theory are shown in Figure 6.

In structure **6a**, the two acid molecules are coplanar which facilitate the formation of two short-range O−H···O interactions ($d_{H\ldots A}$, 1.71 Å). The orientations of the two acid molecules change in the presence of pyridine molecule and one short-range O−H···O ($d_{H\ldots A}$, 1.72 Å) interaction between the two carboxylic acid molecules and another short-range O−H···N ($d_{H\ldots A}$, 1.68 Å) interaction between one acid molecule and pyridine is observed in this case (Figure 6b). Interaction energies of structures **6a** and **6b** with different basis sets are shown in Table 4.

From Table 4 we observed that interaction energy in acid dimer ($E_{\text{int,6a}} = E_{\text{dimer}} − 2E_{\text{acid monomer}}$) with the

Table 4. Interaction Energies (E_{int}) in Acid Dimer (6a) and in the Presence of Pyridine Molecule (6b) (in kcal/mol)

basis sets	in acid dimer ($E_{\text{int,6a}}$)	in presence of pyridine molecule ($E_{\text{int,6b}}$)
6-31+G*	−15.84	−22.84
6-31++G*	−18.16	−25.33
6-31++G**	−18.09	−25.61
AUG-cc-pVDZ	−18.31	−25.40

lower level basis function 6-31+G* is −15.84 kcal/mol, which increases to ∼ −18.0 kcal/mol with higher level basis functions. Calculations with different basis function show that the interaction energy increases by ∼7.0 kcal/mol in the presence of the pyridine, Figure 6b ($E_{\text{int,6b}} = E_{\text{trimer}} − 2E_{\text{acid monomer}} − E_{\text{pyridine}}$). This increase in interaction energy explains the change in orientation of the acid molecules when pyridine is brought into close contact with the formic acid dimer and the hydrogen bonding rearranges to that in **6b**, which is an energetically favored process. A similar observation is made in the solvate **VI** in which the two carboxylic acid groups along with pyridine adopt a geometry stabilized by the O−H···N interactions from one side and C−H···π as well as C−H···O interactions from other sides, which oppose each other to make an optimized geometry.

The solvates of compound **5** and **7** with quinoline (**VII−VIII**) are prepared and characterized (Scheme 3). Part of the crystal structures of quinoline solvates (**VII−VIII**) are shown in Figure 7 and the hydrogen bonding parameters are listed in Table 5.

The quinoline solvate **VII** (1:4 solvate) is analogous to pyridine solvate (**V**) in which quinoline molecules are involved in both discrete and cyclic $R^2_2(7)$ types of hydrogen bonds. There are two discrete O−H···N interactions involving two quinoline molecules and two *trans* carboxylic acid groups of the parent tetra carboxylic acid. Another two cyclic hydrogen bonded quinoline molecules show O2−H2···N2 and C17−H17···O1 interactions and are also placed *trans* to each other around the naphthalene ring.

In solvate **VIII** (1:2 solvate) both quinoline molecules interact with parent dicarboxylic acid via O−H···N [O1−H1···N3 ($d_{d\text{-}A}$, 2.62 Å, and ∠A−H···D, 177.0°) and O3−H3A···N2 ($d_{d\text{-}A}$, 2.70 Å, and ∠A−H···D, 177.9°)] as well as C−H···O [C17−H17···O4 ($d_{d\text{-}A}$, 3.29 Å, and ∠A−H···D, 127.3°) and C26−H26···O2 ($d_{d\text{-}A}$, 3.22 Å, and ∠A−H···D, 121.5°) interactions exhibiting only a cyclic type of hydrogen bond pattern. The quinoline molecules further interact to each other via C−H···π interactions ($d_{C28\ldots\pi}$, 3.61 Å) and to parent dicarboxylic acid also via
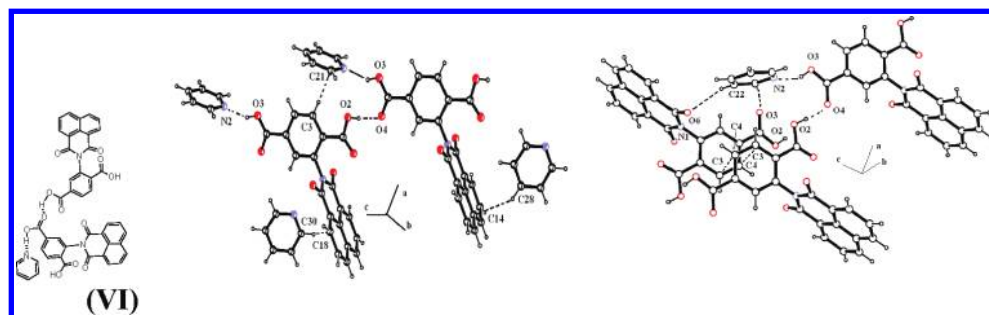
Figure 5. Two different views of a part of the crystal structure of **VI** (drawn with 20%) thermal ellipsoids).
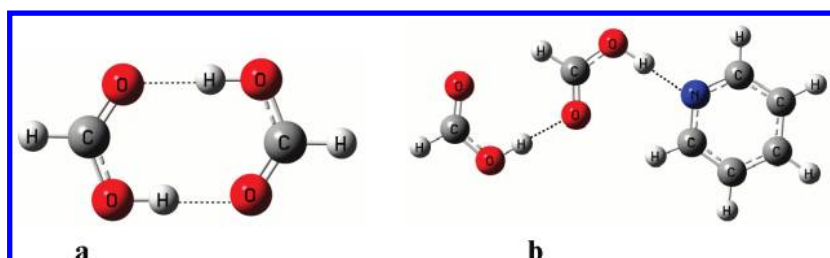

Figure 6. Optimized geometry for (a) formic acid dimer and (b) assembly of pyridine and two formic acids.
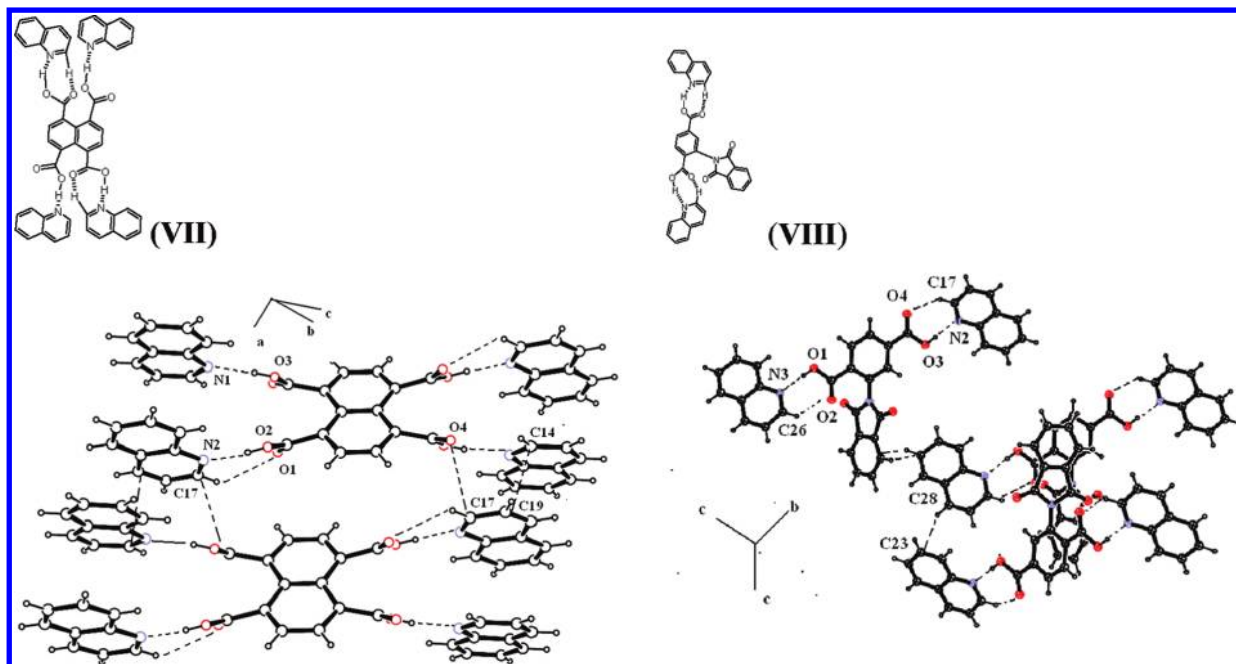

Figure 7. Part of crystal structures of the solvates (**VII**−**VIII**) showing weak interactions among carboxylic acids and quinolines (drawn with 20% thermal ellipsoid).

Table 5. Hydrogen Bond Geometry (Å, °) for the Solvates VII−VIII

compounds	D−H···A	d (D−H)	d (H···A)	d (D···A)	∠D−H···A
VII	O3−H3···N1 [−x + 1, −y + 2, −z + 1]	0.82	1.84	2.66	171.0
	O2−H2···N2 [−x, −y + 1, −z]	1.10	1.80	2.62	174.9
	C17−H17···O2	0.93	2.69	3.29	123.3
VIII	O1−H1···N3 [x + 2, −y + 1, −z + 1]	0.82	1.81	2.62	177.0
	O3−H3A···N2 [x − 1, y, z]	0.82	1.88	2.70	177.9

C−H···π interactions ($d_{C11···\pi}$, 3.78 Å). In the case of quinoline solvates **VII** and **VIII**, there may be another type of cyclic hydrogen bond pattern, namely, QA2 as shown in Figure 1, but in our case, we observed only the QA3 type of cyclic pattern. The QA2 pattern is not observed in these cases possibly due to strong π−π and O−π interactions among the

Table 6. Stability of Different Systems (in kcal/mol)

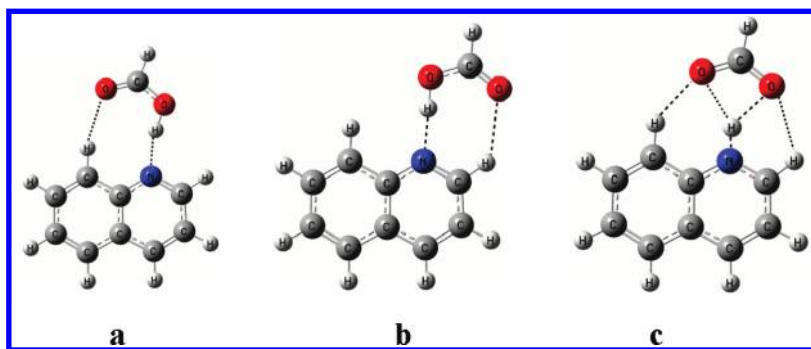| basis sets	stability of **8b** over **8a**	stability of **8b** over **8c**
6-31+G*	−0.57	−13.65
6-31++G*	−0.58	−13.65
6-31++G**	−0.63	−14.87
AUG-cc-pVDZ	−0.54	−14.94

Figure 8. Optimized structure of (a, b) solvates and (c) salt of formic acid with quinoline.

Table 7. Crystallographic Parameters of the Solvates I−VIII

compound no.	I	II	III	IV	V	VI	VII	VIII
formulas	$C_{20}H_{14}N_2O_4$	$C_{24}H_{16}N_2O_4$	$C_{26}H_{19}N_3O_6$	$C_{32}H_{24}N_4O_8$	$C_{34}H_{28}N_4O_8$	$C_{30}H_{21}N_3O_6$	$C_{50}H_{36}N_4O_8$	$C_{34}H_{23}N_3O_6$
formula. wt	346.33	396.39	469.44	592.55	620.60	519.50	820.83	569.55
crystal system	monoclinic	triclinic	monoclinic	triclinic	monoclinic	monoclinic	monoclinic	monoclinic
space group	$P2(1)/c$	$P\bar{1}$	$C2$	$P\bar{1}$	$P2(1)/c$	$C2/c$	$P2(1)/n$	$P2(1)/c$
temperature (K)	296	296	296	296	296	296	296	296
a/Å	17.6509(10)	8.1612(3)	23.7837(11)	7.8269(3)	7.5238(7)	13.2197(13)	7.4716(3)	13.6989(7)
b/Å	12.4017(7)	9.2908(3)	12.7985(5)	13.0543(5)	20.237(2)	14.1173(13)	20.7861(10)	16.5216(8)
c/Å	8.1183(5)	13.3668(4)	3.8331(2)	15.4327(5)	10.1313(9)	27.683(3)	12.8464(6)	12.8230(7)
α/°	90.00	100.934(2)	90.00	102.436(2)	90.00	90.00	90.00	90.00
β/°	102.295(3)	96.943(2)	98.111(4)	100.873(3)	96.131(7)	99.663(8)	96.274(2)	106.265(3)
γ/°	90.00	95.880(2)	90.00	102.566(3)	90.00	90.00	90.00	90.00
V/Å^3	1736.35(18)	979.62(6)	1155.11(9)	1456.36(9)	1533.8(3)	5093.1(8)	1983.17(15)	2786.0(2)
Z	4	2	2	2	2	8	2	4
density/Mg m^{-3}	1.325	1.344	1.350	1.351	1.344	1.355	1.375	1.358
abs coeff /mm^{-1}	0.094	0.093	0.098	0.099	0.097	0.096	0.094	0.095
$F(000)$	720	412	488	616	648	2160	856	1184
total no. of reflections	16803	8143	5439	12590	7914	33859	20241	29891
reflections, $I > 2\sigma(I)$	2406	2056	1835	3119	1461	4554	2294	3671
max 2θ/°	56.52	56.50	50.00	50.00	50.00	56.78	50.22	50.00
ranges (h, k, l)	$-22 \leq h \leq 23$	$-10 \leq h \leq 10$	$-28 \leq h \leq 26$	$-9 \leq h \leq 9$	$-8 \leq h \leq 8$	$-17 \leq h \leq 17$	$-8 \leq h \leq 8$	$-16 \leq h \leq 16$
	$-16 \leq k \leq 16$	$-12 \leq k \leq 12$	$-14 \leq k \leq 14$	$-15 \leq k \leq 15$	$-22 \leq k \leq 24$	$-18 \leq k \leq 18$	$-24 \leq k \leq 24$	$-19 \leq k \leq 19$
	$-10 \leq l \leq 9$	$-17 \leq l \leq 17$	$-4 \leq l \leq 4$	$-18 \leq l \leq 18$	$-11 \leq l \leq 12$	$-36 \leq l \leq 36$	$-15 \leq l \leq 15$	$-13 \leq l \leq 15$
complete to 2θ (%)	98.5	96.1	97.1	90.8	95.6	98.4	99.5	99.8
data/ restraints/parameters	4248/0/236	4654/0/272	1968/1/ 161	4669/0/400	2569/0/210	6285/0/354	3518/0/282	4894/0/390
GOF (F^2)	1.021	1.001	1.050	1.024	1.006	1.059	1.016	1.064
R indices [$I > 2\sigma(I)$]	0.0472	0.0516	0.0310	0.0455	0.0688	0.0509	0.0440	0.0399
R indices (all data)	0.0922	0.1328	0.0338	0.0746	0.1291	0.0725	0.0799	0.0594

Scheme 3. Solvates of Quinoline
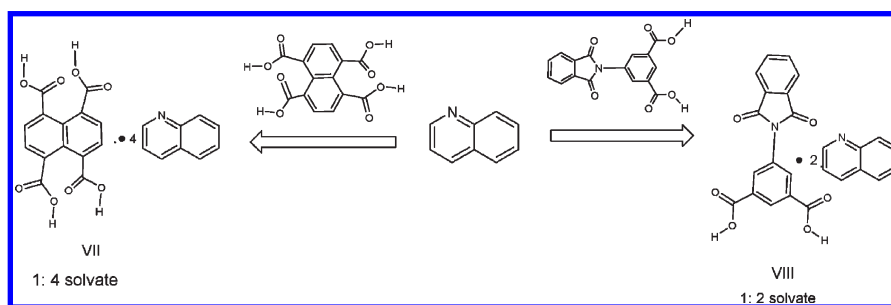
quinoline molecules, but such types of interactions are reported in some related systems.[5b,c]

We have calculated the energy of different hydrogen bond motifs between formic acid and quinoline arising from the different orientations of the carboxylic acid molecule with respect to the quinoline molecule (Figure 8a,b). It is observed that two different short-range O−H···N ($d_{H···A}$, 1.76 Å in **8a**; $d_{H···A}$, 1.73 Å in **8b**) and C−H···O ($d_{H···A}$, 2.35 Å in **8a**; $d_{H···A}$, 2.44 Å in **8b**) interactions exist in structure **8a** and **8b**. The interactions between quinoline and formic acid are exocyclic in **8a**, while these interactions are endocyclic in **8b**. The energy for the formation of quinolinium-carboxylate and

pyridinium-carboxylate salt are also calculated. Our calculations show the possibility of formation of quinolinium-carboxylate salt only. The optimized structure of quinolinium carboxylate salt shown in Figure 8c clearly shows that the two ions are in the same plane. The N−H bond length is found to be 1.06 Å, which is much longer than the typical N−H covalent bond length (0.80 Å). The interaction distance between the H atom of quinolinium cation and the two O atoms of carboxylate anion are 1.81 and 1.99 Å, which shows the formation of the moderately strong hydrogen bond between them. Two C−H···O interactions with $d_{H...A}$ (Å) 2.18 and 2.45 are also exist there. Among the three structures,

8b is found to be the most stable. Stability of **8b** over **8a** and **8c** is shown in Table 6. Different levels of calculations show that the stability of **8b** compared to **8a** lies in the range −0.57 kcal/mol to −0.63 kcal/mol, which also affects the order of N···H bond distances in structures **8a** and **8b** (**8a**, 1.76 Å > **8b**, 1.73 Å). The formation of quinolinium carboxyltae salt (**8c**) is possible, but it is quite unstable compared to **8a** or **8b**. The range of stability of **8b** compared to **8c** with different basis sets is found to be −13.65 kcal/mol to −14.94 kcal/mol. This theoretical data suggest that there are geometrical requirements, which are over and above the conventional pK_a values of an acid under consideration to make solvates or deprotonated species in solid-state assembly.[1a]

Conclusions

A series of structures of pyridine and quinoline solvates of aromatic tetracarboxylic acid and some of the imide tethered carboxylic acids is studied. It is observed that the discrete as well as cyclic types hydrogen bonds are involved with the O−H···N interactions. The presence of different hydrogen bond patterns is governed by the substrates. DFT calculations on energy of different formic acid/pyridine and formic acid/quinoline motifs suggest that the energy differences between these motifs are very small and within the limit of very weak hydrogen bonds. Thus, their formation is controlled by the other weak interactions present in the motifs. These observations are revealed in the experimental structural data, and based on them we could obtain an assembly arising from 1:2 composition of a carboxylic acid with pyridine. This assembly is stabilized by the opposing effect of the weak interactions such as C−H···O to the stronger O−H···N interactions in the crystal structure.

Experimental Section

Computational Details. We have considered motifs derived from formic acid with pyridine or quinoline as model system for calculation of energy. The geometries of the models have been calculated with DFT[9] using the combined Becke's three-parameter exchange functional and the gradient-corrected functional of Lee, Yang and Parr (B3-LYP functional)[10] at 6-31+G* levels. This functional has been demonstrated to predict reliable geometries for hydrogen-bonded systems.[11] Single point calculations at the 6-31+G*, 6-31++G** and B3LYP/AUG-cc-pVDZ[12] level were performed on the fully optimized geometries using B3LYP/6-31+G*. All calculations are performed using the Gaussian03 program.[13] The choice of this basis set is based on the consideration to obtain reliable properties for hydrogen-bonded systems, and it is essential to employ basis sets that possess sufficient diffuseness and angular flexibility.[14] This basis set 6-31++G** is sufficient to predict reliable properties for hydrogen-bonded systems.[11] All calculations are carried out in the gas phase.

Structure Determination. The X-ray single crystal diffraction data were collected at 296 K with MoKα radiation (λ = 0.71073 Å) using a Bruker Nonius SMART CCD diffractometer equipped with a graphite monochromator. The SMART software was used for data collection and also for indexing the reflections and determining the unit cell parameters; the collected data were integrated using SAINT software. The structures were solved by direct methods and refined by full-matrix least-squares calculations using SHELXTL software.[15] All the non-H atoms were refined in the anisotropic approximation against F^2 of all reflections. The H-atoms, except those attached to nitrogen and oxygen atoms, were placed at their calculated positions and refined in the isotropic approximation; those attached to nitrogen and oxygen were located in the difference Fourier maps, and refined with isotropic displacement coefficients. The Crystallographic data collection was done at room temperature and the data are tabulated in Table 7. The

compounds have CCDC numbers 739794, 739795, 739796, 739797, 739798, 739799, 739312 and 739315.

Synthesis and Characterization of Compounds and Their Solvates. The compound naphthalene-1,4,5,8-tetracarboxylic acid was obtained from Sigma Aldrich (USA) and used as received. 2-(1,3-Dioxo-1,3-dihydro-isoindol-2-yl)-benzoic acid: A solution of phthalic anhydride (0.740 g, 5 mmol) and anthranilic acid (0.685 g, 5 mmol) in acetic acid (25 mL) was refluxed for 3 h. The reaction mixture was cooled to room temperature, poured into ice cooled water (50 mL), and stirred for 15 min. A brown colored precipitate of the product was obtained. This was filtered, air-dried. Yield: 85%; IR (KBr, cm^{-1}): 3180 (m), 1725 (s), 1704 (s), 1602 (m), 1493 (w), 1466 (w), 1455 (w), 1384 (m), 1291 (w), 1236 (m), 1218 (m), 1172 (w), 1118 (m), 1084(w), 895 (m), 857 (w), 790 (w), 704 (m), 644 (w), 578 (w). ^{1}H NMR (400 MHz, CDCl$_3$): 8.15 (d, 1H, J = 7.6 Hz), 7.90 (dd, 2H, J = 3.2 Hz), 7.75 (dd, 2H, J = 3.2 Hz), 7.69 (t, 1H, J = 7.6 Hz), 7.53 (t, 1H, J = 7.6 Hz), 7.37 (d, 1H, J = 8.0 Hz). Solvate **I**: The solvate of 2-(1,3-dioxo-1,3-dihydro-isoindol-2-yl)-benzoic acid with pyridine was obtained by crystallizing it from pyridine solution as colorless blocks. IR (KBr, cm^{-1}): 3445 (m), 2928 (w), 1736 (s), 1709 (s), 1606 (w), 1486 (m), 1472 (m), 1385 (s), 1291 (w), 1238 (w), 1176 (w), 1119 (m), 1098 (w), 1006 (w), 883 (w), 811 (m), 793 (w), 718 (m), 531 (w). ^{1}H NMR (400 MHz, CDCl$_3$): 8.67 (d, 2H, J = 4.4 Hz), 8.15 (d, 1H, J = 7.6 Hz), 7.90 (dd, 2H, J = 3.2 Hz), 7.75 (dd, 2H, J = 3.2 Hz), 7.69 (t, 1H, J = 7.6 Hz), 7.53 (t,1H, J = 7.6 Hz), 7.49 (t, 1H, J = 7.2 Hz)7.37 (d,1H, J = 8.0 Hz), 6.43 (bs, 2H). 2-(1,3-dioxo-1H,3H-benzo[*de*]isoquinolin-2-yl)-benzoic acid: Compound 2-(1,3-dioxo-1H,3H-benzo[*de*]isoquinolin-2-yl)-benzoic acid was synthesized by refluxing a solution of 1,8-naphthalic anhydride (0.990 g, 5 mmol) with anthralinic acid (0.685 g, 5 mmol) in acetic acid for 3 h. On cooling, pure crystalline product was obtained. Yield: 82%; IR (KBr, cm^{-1}): 3445 (m), 2858 (w), 1772 (w), 1705 (s), 1679 (s), 1663 (s), 1601 (w), 1588 (m), 1411 (w), 1374 (m), 1356 (m), 1304 (m), 1270 (m), 1237 (s), 1197 (m), 953 (w), 775 (m), 710 (w). ^{1}H NMR (400 MHz, CDCl$_3$): 8.57 (d, 2H, J = 6.8 Hz), 8.23 (d, 2H, J = 8.0 Hz), 8.16 (d, 1H, J = 8.0 Hz), 7.72 (m, 3H), 7.52 (t, 1H, J = 8.0 Hz), 7.32 (d, 1H, J = 8.0 Hz).

Solvate II. The solvate **II** was obtained by crystallization of 2-(1,3-dioxo-1H,3H-benzo[*de*] isoquinolin-2-yl)-benzoic acid in pyridine as colorless blocks. IR (KBr, cm^{-1}): 3476 (m), 2930 (w), 1722 (s), 1698 (s), 1661 (s), 1645 (s), 1622 (m), 1589 (m), 1491 (w), 1438 (w), 1380 (m), 1361 (m), 1244 (s), 1201 (m), 1140 (w), 1079 (w), 847 (w), 780 (m), 710 (w), 515 (w). ^{1}H NMR (400 MHz, CDCl$_3$): 8.60 (d, 2H, J = 7.2 Hz), 8.50 (d, 2H, J = 7.6 Hz), 8.23 (m, 3H), 7.70 (m, 3H), 7.53 (t, 1H, J = 7.6 Hz), 7.34 (d, 1H, J = 7.6 Hz), 7.25 (m, 3H).

5-(1,3-Dioxo-1,3dihydro-isoindol-2-yl)-isophthalic Acid. The compound 5-(1,3-dioxo-1,3-dihydro-isoindol-2-yl)-isophthalic acid was synthesized by refluxing a solution of phthalic anhydride (0.740 g, 5 mmol) and 1-amino 3,5-benzenedicarboxylic acid (0.905 g, 5 mmol) in *N,N*-dimethylformamide for 3 h. On cooling pure crystalline product was obtained. IR(KBr, cm^{-1}): 3445 (m), 2925 (w), 1728 (s), 1605 (w), 1416 (m), 1382 (s), 1281 (s), 1226 (m), 1112 (w), 1081 (w), 875 (w), 759 (m), 711 (s), 641 (w), 530 (w). ^{1}H NMR (400 MHz, DMSO-d_6): 8.49 (s, 1H), 8.28 (s, 2H), 7.99 (dd, 2H J = 3.2 Hz), 7.91 (dd, 2H J = 3.2 Hz). Solvate **III**: The solvate III was obtained by crystallization of 5-(1,3 dioxo-1,3dihydro-isoindol-2-yl)-isophthalic acid in pyridine as colorless blocks. IR (KBr cm^{-1}): 3451 (m), 3083 (w), 2854 (w), 1716 (s), 1605 (m), 1427 (m), 1382 (s), 1283 (s), 1226 (m), 1114 (m), 921 (w), 758 (w), 712 (w), 691 (w), 642 (w), 530 (w). ^{1}HNMR (400 MHz, DMSO-d_6): 8.52 (bs, 4H), 8.49 (s, 1H), 8.28 (s, 2H), 7.99 (dd, 2H J = 3.2 Hz), 7.91 (dd, 2H J = 3.2 Hz) 7.89 (t, 2H, J = 6.8 Hz), 7.39 (bs, 4H). 2-(5-carboxy-1,3-dioxo-1,3-dihydro-isoindol-2-yl)-terephthalic acid: This compound was synthesized by refluxing a solution of 1,3-dioxo-1,3-dihydro-isobenzofuran-5-carboxylic acid (0.960 g, 5 mmol) and 1-amino 2,4-benzene dicarboxylic acid (0.905 g, 5 mmol) in acetic acid for 4 h. On cooling, pure crystalline product was obtained. Yield: 84%; IR (KBr, cm^{-1}): 3425 (m), 2899 (m), 2661 (m), 1786 (w), 1709 (s), 1572 (w), 1498 (w), 1445 (m), 1416 (m), 1298 (s), 1274 (s), 1220 (m), 1111 (m), 866 (w), 753 (w), 727 (w), 608 (w), 529 (w). ^{1}HNMR (400 MHz, DMSO-d_6): 8.44 (d, 1H, J = 7.6 Hz), 8.33 (s, 1H), 8.15 (s, 2H), 8.12 (d, 1H, J = 4.0 Hz), 8.11 (s, 1H). Solvate **IV**: Solvate **IV** was obtained as colorless blocks from the pyridine solution of the compound 2-(5-carboxy-1,3-dioxo-1,3-dihydro-isoindol-2-yl)-terephthalic acid.

IR (KBr cm^{-1}): 3445 (m), 3064 (w), 2461(w), 1778 (m), 1716 (s), 1599 (m), 1489 (w), 1423(m), 1373 (m), 1286 (s), 1251(s), 1209 (s), 1121(m), 1101 (m), 1061(m), 1007 (w), 758 (m), 729 (w), 636 (w), 573(w). ^{1}HNMR (400 MHz, DMSO-d_6): 8.58 (d, 6H, *J* = 4.0 Hz), 8.45 (d, 1H, *J* = 7.6 Hz), 8.35 (s, 1H), 8.16 (s, 2H), 8.13 (d, 1H, *J* = 3.6 Hz), 8.11 (s, 1H), 7.83 (t, 3H), 7.38 (t, 6H). Solvate **V**: Solvate **V** was obtained as colorless blocks from the pyridine solution of naphthalene-1,4,5,8-tetracarboxylic acid. IR (KBr, cm^{-1}): 3416 (m), 2928 (w), 2772 (w), 2381(m), 1706 (s), 1599 (w), 1501(m), 1385(m), 1284 (s), 1196 (s), 872 (w), 805 (m), 778 (m), 670 (w). ^{1}HNMR (400 MHz, DMSO-d_6): 8.56 (d, 8H, *J* = 8.0 Hz), 8.05 (s, 4H), 7.76 (m, 8H), 7.38 (t, 4H, 6.4 Hz). 2-(1,3-Dioxo-1*H*,3*H*-benzo[de]isoquinolin-2-yl)-terephthalic acid: This compound was synthesized by refluxing a solution of 1,8-naphthalic anhydride (0.990 g, 5 mmol) and 1-amino 2,4-benzenedicarboxylic acid (0.905 g, 5 mmol) in *N*,*N*-dimethylformamide. IR (KBr cm^{-1}): 3436 (s), 2923 (w), 1710 (s), 1659 (s), 1591 (m), 1498 (w), 1438 (w), 1406 (w), 1380 (m), 1281 (s), 1248 (s), 1204 (m), 1120 (w), 1069 (w), 1017 (m), 952 (w), 886 (w), 850 (w), 780 (m), 769 (m), 709 (w), 535 (w). ^{1}H NMR (400 MHz, DMSO-d_6): 8.53 (dd, 4H, *J* = 7.2 Hz), 8.19 (d, 1H, *J* = 8.4 Hz), 8.13 (d, 1H, *J* = 8.0 Hz), 8.08 (s, 1H), 7.92 (t, 2H, *J* = 8.0 Hz). Solvate **VI**: The solvate **VI** was obtained as colorless blocks from the pyridine solution of compound 2-(1,3-dioxo-1*H*,3*H*-benzo[de]isoquinolin-2-yl)-terephthalic acid. IR (KBr, cm^{-1}): 3446 (m), 3074 (w), 2474 (w), 1702 (s), 1661(s), 1588 (m), 1491(w), 1374 (m), 1245 (s), 1162 (m), 949 (w), 892 (w), 774 (m), 703 (w), 591(w). ^{1}HNMR (400 MHz, DMSO-d_6): 8.57 (d, 4H, *J* = 3.2 Hz), 8.52 (dd, 4H, *J* = 6.0 Hz), 8.21 (d, 1H, *J* = 8.4 Hz), 8.15 (d, 1H, *J* = 8.4 Hz), 8.10 (s, 1H), 7.91 (t, 2H, *J* = 8.0 Hz), 7.78 (t, 2H, *J* = 7.6 Hz), 7.37 (m, 2H). Solvate **VII**: Solvate **VII** was obtained from a solution of naphthalene-1,4,5,8-tetracarboxylic acid in quinoline as colorless blocks. IR (KBr, cm^{-1}): 3432 (m), 2381(m), 1926 (w), 1704 (s), 1597 (m), 1504 (m), 1396 (m), 1274 (s), 1188 (s), 872 (w), 805 (m), 775 (m), 670 (w). ^{1}H NMR (400 MHz, DMSO-d_6): 8.91 (d, 4H, *J* = 4.0 Hz), 8.37 (d, 4H, *J* = 8.0 Hz), 8.01 (m, 12H), 7.77 (t, 4H, *J* = 6.8 Hz), 7.61 (t, 4H, *J* = 6.8 Hz), 7.53 (dd, 4H, *J* = 4.0 Hz). 2-(1,3dioxo-1,3-dihydro-isoindol-2-yl)-terephthalic acid: Compound 2-(1,3dioxo-1,3-dihydro-isoindol-2-yl)-terephthalic acid was synthesized by refluxing a solution of phthalic anhydride (0.740 g, 5 mmol) and 1-amino 2,4-benzene dicaboxylic acid (0.905 g, 5 mmol) in acetic acid for 3 h. Yield: 87%; IR (KBr, cm^{-1}): 3082 (m), 2644 (w), 1694 (s), 1444 (s), 1376 (m), 1292 (m), 1250 (s), 1175 (w), 1140 (w), 1118 (m), 946 (w), 883 (w), 792 (w), 759 (m), 725 (w), 529 (w). ^{1}H NMR (400 MHz, DMSO-d_6): 8.13 (s, 2H), 8.10 (s,1H), 7.99 (dd,2H, *J* = 3.2 Hz), 7.93 (dd, 2H, *J* = 3.2 Hz). Solvate **VIII**: Solvate **VIII** was obtained as colorless blocks from the quinoline solution of compound 2-(1,3 dioxo-1,3-dihydro-isoindol-2-yl)-terephthalic acid. IR (KBr, cm^{-1}): 3463 (m), 2788 (w), 2449 (m), 1774 (w), 1715 (s), 1496 (m), 1473 (w), 1459 (w), 1421 (m), 1376 (m), 1282 (s), 1234 (m), 1216 (m), 1141 (w), 1120 (m), 881(w), 809 (m), 785 (m), 720 (w), 636 (w), 528 (w). ^{1}HNMR (400 MHz, DMSO-d_6): 8.90 (dd, 2H, *J* = 3.2 Hz), 8.37(d, 2H, *J* = 7.6 Hz), 8.14 (s, 2H), 8.11 (s, 1H), 8.00 (m, 6H), 7.92 (dd, 2H, *J* = 3.2 Hz), 7.75 (t, 2H, *J* = 7.2 Hz), 7.61 (t, 2H, *J* = 6.8 Hz), 7.53 (dd, 2H, *J* = 4.0 Hz).

Supporting Information Available: Crystallographic information files are available free of charge via the Internet at http://pubs.acs.org.

References

(1) (a) Mohamed, S.; Tocher, D. A.; Vickers, M.; Karamertzanis, P. G.; Price, S. L. *Cryst. Growth Des.* **2009**, *9*, 2881. (b) Bhogala, B R.; Basavoju, S.; Nangia, A. *Cryst. Growth and Des.* **2005**, *5*, 1683. (c) Bhogala, B R.; Nangia, A. *Cryst. Growth Des.* **2003**, *3*, 547. (d) Biradha, K.; Zaworotoko, M. J. *Cryst. Eng.* **1998**, *1*, 67. (e) Blagden, N.; de Matas, M.; Gavan, P. T.; York, P. *Adv. Drug Delivery Rev.* **2007**, *59*, 617. (f) Steiner, T. *Angew. Chem., Int. Ed. Engl.* **2002**, *41*, 48.

(2) (a) Bhatt, P. M.; Ravindra, N. V.; Banerjee, R.; Desiraju, G. R. *Chem. Commun.* **2005**, 1073. (b) Visheswar, A. P.; McMahon, J. A.; Bis, J. A.; Zaworotoko, M. J. *J. Pharm. Sci.* **2006**, *95*, 499. (c) Morissette, S. L.; Almarsson, O.; Peterson, M. L.; Remenar, J. F.; Read, M. J.; Lemmo, A. V.; Ellis, S.; Cima, M. J.; Gardner, C. R. *Adv. Drug Delivery Rev.* **2004**, *56*, 275. (d) Weyna, D. R.; Shattock, T.; Visweshwar, P.; Zaworotko, M. J. *Cryst. Growth Des.* **2009**, *9*, 1106.

(3) (a) Lim, S.; Kim, H.; Selvapalam, N.; Kim, K. J.; Cho, S. J.; Seo, G.; Kim, K. *Angew. Chem., Int. Ed. Engl.* **2008**, *47*, 3352. (b) Rajput, L.; Biradha, K. *Cryst. Growth Des.* **2009**, *9*, 40. (c) Rajput, L.; Biradha, K. *J. Mol. Struct.* **2008**, *876*, 339. (d) Msayib, K. J.; Book, D.; Budd, P. M.; Chaukura, N.; Harris, K. D. M.; Helliwell, M.; Tedds, S.; Walton, A.; Warren, J. E.; Xu, M.; McKeown, N. B. *Angew. Chem., Int. Ed. Engl.* **2009**, *48*, 3273.

(4) (a) Kinbara, K.; Hashimoto, Y.; Sukegawa, M.; Nohira, H.; Saigo, K. *J. Am. Chem. Soc.* **1996**, *118*, 3441. (b) Seaton, C. C.; Parkin, A.; Wilson, C. C.; Bladen, N. *Cryst. Growth Des.* **2009**, *9*, 47. (c) Shatock, T. R.; Arora, K. K.; Visheshwar, P.; Zaworotko, M. J. *Cryst Growth Des.* **2008**, *8*, 4533. (d) Sudhakar, P.; Srivijaya, R.; Sreekanth, B. R.; Jayanthi, P. K.; Vishweshar, P.; Babu, M. J.; Vyas, K.; Iqbal, J. *J. Mol. Struct.* **2008**, *885*, 45. (e) Balevicius, V.; Bariseviciute, R.; Aidas, K.; Svoboda, I.; Ehreberg, H.; Fuess, H. *Phys. Chem. Chem. Phys.* **2007**, *9*, 3181. (f) Jin, J. M.; Hu, M. L.; Xuan, R. C.; Yu, K. B. *J. Chem. Cryst.* **2004**, *34*, 657. (g) Carrow, C. J.; Wheeler, K. A. *Mater. Res. Bull.* **1998**, 283.

(5) (a) Cheney, M. L.; McManus, G. J.; Perman, J. A.; Wang, Z.; Zaworotko, M. J. *Cryst. Growth Des.* **2007**, *7*, 616. (b) Singh, D.; Baruah, J. B. *CrystEngComm* doi:10.1039/b911084d. (c) Shan, N.; Batchelor, E.; Jones, W. *Tetrahedron Lett.* **2002**, *43*, 8721.

(6) (a) Singh, W. M.; Barooah, N.; Baruah, J. B. *J. Mol. Struct.* **2008**, *875*, 329. (b) Haynes, D. A.; Jones, W.; Motherwell, W. D. S. *CrystEngComm* **2006**, *8*, 830.

(7) (a) Stanton, M. K.; Bak, A. *Cryst. Growth Des.* **2008**, *8*, 3856. (b) Bhogala, B. R.; Basavoju, S.; Nangia, A. *CrystEngComm* **2005**, *7*, 551. (c) Vishweshwar, P.; Nangia, A.; Lynch, V. M. *Cryst. Growth Des.* **2003**, *3*, 783. (d) Karki, S.; Friscic, T.; Jones, W. *CrystEngComm* **2009**, *11*, 470.

(8) (a) Barooah, N.; Sarma, R. J.; Baruah, J. B. *Cryst. Growth Des.* **2003**, *3*, 639. (b) Degenhardt, C., III; Shortell, D. B.; Adams, R. D.; Simizu, K. D. *Chem. Commun.* **2000**, 920. (c) Degenhardt, C., III; Lavin, J. M.; Smith, D. M.; Simizu, K. D. *Org. Lett.* **2005**, *7*, 4079. (d) Kishikawa, K.; Iwashima, C.; Yamguchi, K.; Yamamoto, M. *J. Chem. Soc. Perkin. Trans. 1* **2000**, 2217. (e) Kishikawa, K.; Tsubokura, S.; Kohomoto, S.; Yamamoto, M. *J. Org. Chem.* **1999**, *64*, 7568.

(9) (a) Ireta, J.; Neugebauer, J.; Scheffler, M. *J. Phys. Chem. A* **2004**, *108*, 5692. (b) Korth, H. G.; de Heer, M. I.; Mulder, P. *J. Phys. Chem. A* **2002**, *106*, 8779. (c) Hohenberg, P.; Kohn, W. *Phys. Rev. B* **1964**, *136*, 864.

(10) (a) Becke, A. D. *J. Chem. Phys.* **1993**, *98*, 5648. (b) Lee, C.; Yang, W.; Parr, R. G. *Phys. Rev. B* **1988**, *37*, 785.

(11) (a) Dkhissi, A.; Adamowicz, L.; Maes, G. *J. Phys. Chem. A* **2000**, *104*, 2112. (b) Dkhissi, A.; Adamowicz, L.; Maes, G. *Chem. Phys. Lett.* **2000**, *324*, 127.

(12) Woon, D. E; Dunning, T. H., Jr. *J. Chem. Phys.* **1993**, *98*, 1358.

(13) (a) *GAUSSIAN03, Revision B.05*; Gaussian, Inc.: Pittsburgh, PA, 2003. (b) *GAUSSIAN03, Revision B.05*; Gaussian, Inc.: Pittsburgh, PA, 2003.

(14) Chalasinski, G.; Szczesniak, M. *Chem. Rev.* **1994**, *94*, 1723.

(15) Sheldrick, G. M. *Acta Crystallogr.* **2008**, *A64*, 112.